

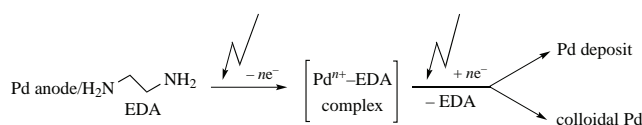
# The first example of anodic corrosion of Pd in aqueous ethylenediamine with formation of colloidal palladium

Marina D. Vedenyapina,\* Vladimir V. Kuznetsov, Stanislav A. Kulaishin,  
 Nina N. Makhova\* and Marina M. Kazakova

*N. D. Zelinsky Institute of Organic Chemistry, Russian Academy of Sciences, 119991 Moscow, Russian Federation. Fax: +7 499 135 5328; e-mail: mvedenyapina@yandex.ru*

DOI: 10.1016/j.mencom.2021.09.015

For the first time, corrosion of a Pd anode was detected during electrolysis in a weakly alkaline aqueous solution of ethylenediamine. The kinetics and mechanism of the process were investigated by the methods of cyclic voltammetry and gravimetry. Scanning electron microscopy showed corrosion of the Pd anode and deposition of Pd on the cathode surface, while the formation of colloidal Pd in the working solution was identified by transmission electron microscopy.



**Keywords:** palladium anode, corrosion, ethylenediamine, kinetics, voltammetry, gravimetry, colloidal Pd, electron microscopy.

Palladium catalysts play a significant role in modern chemical science and industry. Outstanding contributions to the C–C coupling reaction in organic synthesis catalyzed by Pd derivatives<sup>1,2</sup> were made by Suzuki, Heck and Negishi, who received the 2010 Nobel Prize in Chemistry. Palladium catalysts are widely used in petroleum cracking,<sup>3</sup> catalytic combustion of methane,<sup>4</sup> CO oxidation,<sup>5</sup> alcohol oxidation,<sup>6,7</sup> selective hydrogenation of unsaturated hydrocarbons<sup>8,9</sup> and dehydrogenation of alkanes.<sup>10</sup>

With the development of nanoscience and technology, bimetallic catalysts have been synthesized based on a combination of palladium with various metals (Pt, Au, Ag, Pb, Ga, In, Nb, Ru and Zn); this provided more opportunities for optimizing catalytic performance compared to monometallic palladium catalysts.<sup>11–13</sup> Recently, the application of palladium-based bimetallic catalysts has been expanded in the emerging field of renewable energy conversion.<sup>14–18</sup> A bimetallic nanocatalyst based on palladium (for example, Au–Pd) was prepared by the standard colloidal method, including the reduction of a mixture of an aqueous solution of HAuCl<sub>4</sub> and an acidic solution of PdCl<sub>2</sub> with NaBH<sub>4</sub> in water, followed by immobilization of the resulting dark red colloid on TiO<sub>2</sub> or activated carbon and drying at 110 °C for 16 h.<sup>19</sup> A rather original approach to creating complex-shaped palladium nanoparticles (star-shaped concave icosahedra, pentatwinned rods and bipyramids) is presented.<sup>20</sup> An unusual cathodic corrosion method for producing nanocrystals of individual precious metals and their alloys is described.<sup>21</sup> Since colloidal palladium is widely used for various purposes,<sup>22</sup> the search for milder and more facile methods for its preparation remains highly urgent.

We recently found that corrosion of the gold anode under galvanostatic conditions in the presence of aliphatic diamines, such as ethylenediamine (EDA), 1,2-diaminopropane, 1,3-diaminopropane and 1,4-diaminobutane, as ligands in a weakly alkaline aqueous medium results in the electrolytic deposition of gold on platinum or iron cathode. The process was monitored using cyclic voltammetry with a low potential scan rate

(1 mV s<sup>-1</sup>); EDA was the most effective.<sup>23,24</sup> Evidently, the process begins with forming a complex of gold with a diamine at the anode, which is transferred into the solution and reduced at the cathode with the deposition of gold on its surface. Later, these processes were investigated in more detail by voltammetric and gravimetric methods. It was found that electrolysis using a gold anode in a medium of branched-chain diamines gives, along with the electrolytic deposition of gold on the cathode, colloidal gold in an electrolytic solution.<sup>25–27</sup> This result made it possible to assume that similar processes can also be realized for anodic corrosion of other metals, particularly palladium.

This work aimed to study the anodic corrosion of palladium under galvanostatic conditions in a weakly basic medium in the presence of EDA as a ligand, resulting in the electrolytic deposition of palladium on a steel wire cathode and the formation of colloidal palladium in the electrolyte medium.

The study of anodic corrosion of palladium was carried out using EDA as a ligand (for details, see Online Supplementary Materials) since it was the most active in transferring gold from the anode to the cathode compared to other aliphatic diamines.<sup>23</sup> The electrolysis was investigated using cyclic voltammetry in a 0.1 M EDA solution in a 0.05 M aqueous solution of K<sub>2</sub>CO<sub>3</sub> as a supporting electrolyte. Cyclic voltammograms (CVs) were recorded in the potential range  $E = 0–1200$  mV at different potential scan rates [Figure 1(a)]. The peaks on the anodic branches of the CV curves at potentials of about 800 mV were poorly resolved. The intensity of the current peaks ( $I_{p,a}$ ) increased with an increase in the potential scan rate, confirming the Pd–EDA complex formation. During the reverse scanning of the potential, small peaks at potentials  $E = 100–350$  mV were detected on the cathodic branches of the CV curves (steel cathode), which attests to the reduction of the products of anodic corrosion of Pd. No  $I_{p,a}$  was present in the CV curve recorded in the supporting electrolyte without EDA in the same potential range.

Due to the high value of the maximum current potential on the anodic branch of the CV curve, the stoichiometry of the

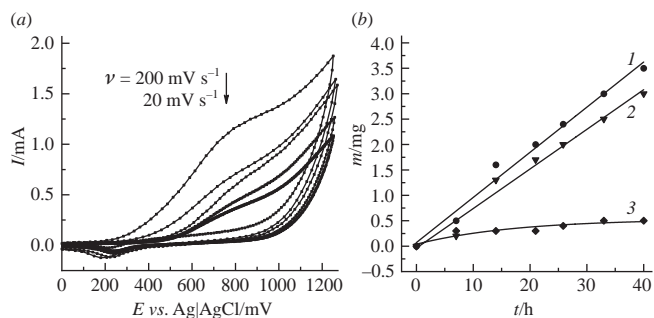


**Figure 1** (a) CV curves of Pd anode in 0.1 M EDA solution in 0.05 M aqueous solution of  $K_2CO_3$  at potential scan rates ( $\nu$ ) of 200, 125, 100, 50 and 20  $mV s^{-1}$ . (b) The time dependences of Pd anode dissolution and cathode mass increase in the 0.1 M EDA solution at a current of 10 mA: (1) mass loss of the Pd anode ( $m_{corr}$ ), (2) calculated mass of Pd in solution ( $m_{sol}$ ) and (3) mass of the cathode deposit of Pd ( $m_{dep}$ ).

anodic process cannot be determined directly. Probably, the anodic process is multielectron, and each anodic CV peak in the ligand solution is actually the sum of the peaks corresponding to the transfer of single electrons. An indirect confirmation of this assumption is the absence of a clear linear dependence of  $I_{p,a}$  on the potential scan rate for the anodic process.

The cathodic current peaks ( $I_{p,c}$ ) linearly depend on the potential scan rate (Figure S1, see Online Supplementary Materials). Evidently, the reduction of Pd anodic corrosion products occurs directly on the cathode surface, with electron transfer being the rate-limiting step. In this case, the Laviron equation<sup>28</sup> can be applied [equation (1)].

$$I_{p,c} = nFQ\nu/4RT, \quad (1)$$

where  $n$  is the number of electrons participating in the reaction with one molecule,  $F$  is the Faraday constant ( $96485 C mol^{-1}$ ),  $Q$  is the charge corresponding to the peak area in the cathodic branch of the CV,  $\nu$  is the potential scan rate ( $mV s^{-1}$ ),  $R$  is the gas constant ( $8.314 J mol^{-1} K^{-1}$ ) and  $T$  is the absolute temperature.

The number of electrons  $n$  participating in the cathodic process in the range of  $\nu = 20\text{--}200 mV s^{-1}$ , calculated using the Laviron equation, was 1.84–2.15. Therefore, in the cathodic reduction of Pd anodic corrosion products in the EDA solution, two electrons are involved.

Electrolysis under galvanostatic conditions using a Pd anode was carried out in a 1.0 M solution of EDA in a 0.05 M aqueous solution of  $K_2CO_3$  for two current values of 5 and 10 mA to determine the effect of the current on the corrosion process. As in the case of anodic corrosion of Au, gravimetric measurements of the anode and cathode showed a loss in mass of the Pd anode and an increase in the cathode mass. Obviously, in the course of the process, a Pd–EDA complex is formed at the anode, then it migrates into the solution and subsequently is reduced at the cathode, with Pd metal being deposited on the cathode surface. The time dependences of the Pd anode mass loss ( $m_{corr}$ ) and the increase in a cathodic deposition ( $m_{dep}$ ) for a current of 10 mA are presented in Figure 1(b), while the same dependences for a current of 5 mA are shown in Figure S2. The difference between the  $m_{corr}$  and  $m_{dep}$  values was used to calculate the mass of Pd in the electrolyte solution ( $m_{sol}$ ). According to Figures 1(b) and S2, the values of  $m_{corr}$ ,  $m_{dep}$  and  $m_{sol}$  increase monotonically. To interpret the kinetics of the process, we can represent the sum of anodic dissolution and cathodic deposition of Pd as a system of differential equations:

$$dm_1/dt = k_1, \quad (2)$$

$$dm_2/dt = k_1 - k_2m_2, \quad (3)$$

$$dm_3/dt = k_2m_2, \quad (4)$$

**Table 1** Comparison of the kinetic parameters of anodic corrosion of Pd in a solution of EDA and Au in solutions of EDA<sup>22</sup> and 2,2-dimethyl-1,3-diaminopropane.<sup>24</sup>

Metal	Diaminoalkane	$k_1/mg h^{-1}$		$k_2/h^{-1}$	
		10 mA	5 mA	10 mA	5 mA
Pd	EDA	0.0875	0.0500	0.0071	0.0025
Au	EDA	0.55	–	0.11	–
Au	2,2-Dimethyl-1,3-diaminopropane	0.09	–	0.02	–

where  $m_1$  is  $m_{corr}$ ,  $m_2$  is  $m_{sol}$  and  $m_3$  is  $m_{dep}$ . The solution of this system of equations using the Mathcad program made it possible to find  $k_1$  and  $k_2$  that most accurately describe the obtained experimental data presented in Figures 1(b) and S2. The constants  $k_1$  and  $k_2$  for the Pd anode in an EDA solution for currents of 5 and 10 mA are summarized in Table 1.

Comparison of the data in Table 1 with the known results<sup>24</sup> on the corrosion of the gold anode showed that in the EDA solution, the corrosion of Pd proceeds with more difficulty than the corrosion of the gold anode. Comparable  $k_1$  values were found for Pd corrosion in an EDA solution and Au corrosion in a 2,2-dimethyl-1,3-diaminopropane solution.<sup>26</sup> The  $k_2$  values corresponding to the deposition of metals on the cathode were different.

After completing the anodic corrosion of Pd in a weakly alkaline solution of EDA for 40 h, the anode and cathode were examined using a scanning electron microscope, and the electrolyte was studied using a transmission electron microscope. Electron microscopy studies have shown that during electrolysis, the Pd anode undergoes corrosion [Figure 2(a)], and Pd is deposited on the surface of the steel cathode in the form of globules [Figure 2(b)]. The analysis of the chemical composition of the steel cathode by energy-dispersive X-ray spectroscopy (EDX) demonstrated the presence of Pd on the surface [Figure 2(c)].

Colloidal palladium particles with a round shape and a size of 10–40 nm were detected in the working solution (electrolyte) using transmission electron microscopy after the end of electrolysis at a current of 10 mA [Figure 2(d)]. Fewer Pd colloidal particles with a smaller size (5–20 nm) were found in the transmission electron microscope image after electrolysis at a current of 5 mA (Figure S3). These results correlate with the results of gravimetric measurements [Figures 1(b) and S2].

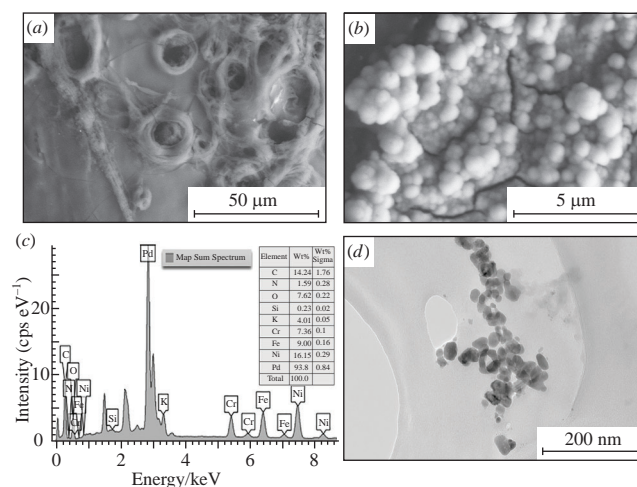


**Figure 2** Scanning electron microscope images of (a) Pd anode surface and (b) steel cathode surface after electrolysis in EDA solution. (c) EDX spectrum and elemental composition of the steel cathode surface after electrolysis with Pd anode. (d) Transmission electron microscope image of the electrolyte after anodic corrosion of Pd in EDA solution at 10 mA current.

In conclusion, we first investigated the electrochemical behavior of a palladium anode under galvanostatic conditions in a weakly alkaline aqueous solution of EDA, a representative of aliphatic diamines, and found anodic corrosion of Pd. Evidently, corrosion occurs *via* the formation of a Pd–EDA complex (cyclic voltammetry data) at the anode, followed by the migration of this complex into solution and subsequent reduction on the cathode surface to give a compact Pd deposit and nanosized colloidal Pd in an electrolyte medium. These results were recorded in the form of micrographs using scanning and transmission electron microscopes. The kinetics of the anodic dissolution, cathodic deposition and transfer of Pd into the EDA solution at currents of 5 and 10 mA was studied by the gravimetric method. It was found that the anodic corrosion of Pd in the EDA solution proceeds with more difficulty than the corrosion of the Au anode under the same conditions. As far as we know, this is the first example of Pd anode corrosion leading to colloidal Pd.

The work was financially supported by the Science Schools Department Program of the N. D. Zelinsky Institute of Organic Chemistry of the Russian Academy of Sciences. The authors are grateful to the Department of Structural Research of the N. D. Zelinsky Institute of Organic Chemistry of the Russian Academy of Sciences for carrying out electron microscopy of the samples.

#### Online Supplementary Materials

Supplementary data associated with this article can be found in the online version at doi: 10.1016/j.mencom.2021.09.015.

#### References

- N. Miyaura and A. Suzuki, *Chem. Rev.*, 1995, **95**, 2457.
- H. Li, C. C. Johansson Seechurn and T. J. Colacot, *ACS Catal.*, 2012, **2**, 1147.
- J. Wildschut, F. H. Mahfud, R. H. Venderbosch and H. J. Heeres, *Ind. Eng. Chem. Res.*, 2009, **48**, 10324.
- R. J. Bunting, X. Cheng, J. Thompson and P. Hu, *ACS Catal.*, 2019, **9**, 10317.
- G. Spezzati, A. D. Benavidez, A. T. DeLaRiva, Y. Su, J. P. Hofmann, S. Asahina, E. J. Olivier, J. H. Neethling, J. T. Miller, A. K. Datye and E. J. M. Hensen, *Appl. Catal., B*, 2019, **243**, 36.
- D. I. Enache, J. K. Edwards, P. Landon, B. Solsona-Espriu, A. F. Carley, A. A. Herzing, M. Watanabe, C. J. Kiely, D. W. Knight and G. J. Hutchings, *Science*, 2006, **311**, 362.
- J. Feng, C. Ma, P. J. Miedziak, J. K. Edwards, G. L. Brett, D. Li, Y. Du, D. J. Morgan and G. J. Hutchings, *Dalton Trans.*, 2013, **42**, 14498.
- G. Vilé, D. Albani, N. Almora-Barrios, N. López and J. Pérez-Ramírez, *ChemCatChem*, 2016, **8**, 21.
- C. W. A. Chan, A. H. Mahadi, M. M.-J. Li, E. C. Corbos, C. Tang, G. Jones, W. C. H. Kuo, J. Cookson, C. M. Brown, P. T. Bishop and S. C. Edman Tsang, *Nat. Commun.*, 2014, **5**, 5787.
- Z. Ma, Z. Wu and J. T. Miller, *Catal., Struct. React.*, 2017, **3**, 43.
- J. Fan, H. Du, Y. Zhao, Q. Wang, Y. Liu, D. Li and J. Feng, *ACS Catal.*, 2020, **10**, 13560.
- M. Sankar, N. Dimitratos, P. J. Miedziak, P. P. Wells, C. J. Kiely and G. J. Hutchings, *Chem. Soc. Rev.*, 2012, **41**, 8099.
- L. Zhang, Z. Xie and J. Gong, *Chem. Soc. Rev.*, 2016, **45**, 3916.
- D. Kan, D. Wang, X. Zhang, R. Lian, J. Xu, G. Chen and Y. Wei, *J. Mater. Chem. A*, 2020, **8**, 3097.
- X. Qin, L. Zhang, G.-L. Xu, S. Zhu, Q. Wang, M. Gu, X. Zhang, C. Sun, P. B. Balbuena, K. Amine and M. Shao, *ACS Catal.*, 2019, **9**, 9614.
- X. Wu, Y. Jiang, Y. Yan, X. Li, S. Luo, J. Huang, J. Li, R. Shen, D. Yang and H. Zhang, *Adv. Sci.*, 2019, **6**, 1902249.
- Z. Nodehi, A. A. Rafati and A. Ghaffarinejad, *Appl. Catal., A*, 2018, **554**, 24.
- M. Cui, G. Johnson, Z. Zhang, S. Li, S. Hwang, X. Zhang and S. Zhang, *Nanoscale*, 2020, **12**, 14068.
- S. J. Freakley, N. Agarwal, R. U. McVicker, S. Althahban, R. J. Lewis, D. J. Morgan, N. Dimitratos, C. J. Kiely and G. J. Hutchings, *Catal. Sci. Technol.*, 2020, **10**, 5935.
- S. P. McDarby, C. J. Wang, M. E. King and M. L. Personick, *J. Am. Chem. Soc.*, 2020, **142**, 21322.
- J. Feng, D. Chen, A. S. Sediq, S. Romeijn, F. D. Tichelaar, W. Jiskoot, J. Yang and M. T. M. Koper, *ACS Appl. Mater. Interfaces*, 2018, **10**, 9532.
- M. A. Mahdaly, J. S. Zhu, V. Nguyen and Y.-S. Shon, *ACS Omega*, 2019, **4**, 20819.
- M. D. Vedenyapina, V. V. Kuznetsov, D. I. Rodikova, N. N. Makhova and A. A. Vedenyapin, *Mendeleev Commun.*, 2018, **28**, 181.
- M. D. Vedenyapina, V. V. Kuznetsov, N. N. Makhova and D. I. Rodikova, *Russ. J. Phys. Chem. A*, 2019, **93**, 466 (*Zh. Fiz. Khim.*, 2019, **93**, 381).
- M. D. Vedenyapina, G. Ts. Ubushieva, V. V. Kuznetsov, N. N. Makhova and A. A. Vedenyapin, *Russ. J. Phys. Chem. A*, 2016, **90**, 2312 (*Zh. Fiz. Khim.*, 2016, **90**, 1748).
- M. D. Vedenyapina, V. V. Kuznetsov, A. S. Dmitrenok, M. E. Minyaev, N. N. Makhova and M. M. Kazakova, *Russ. Chem. Bull., Int. Ed.*, 2021, **70**, 735 (*Izv. Akad. Nauk, Ser. Khim.*, 2021, 735).
- M. D. Vedenyapina, V. V. Kuznetsov, N. N. Makhova and D. I. Rodikova, *Russ. Chem. Bull., Int. Ed.*, 2020, **69**, 1884 (*Izv. Akad. Nauk, Ser. Khim.*, 2020, 1884).
- E. Laviron, *J. Electroanal. Chem. Interfacial Electrochem.*, 1979, **101**, 19.

Received: 14th April 2021; Com. 21/6523